Functional Organization of Ferret Auditory Cortex

Jennifer K. Bizley[1], Fernando R. Nodal[1], Israel Nelken[2] and
Andrew J. King[1]

[1]University Laboratory of Physiology, Parks Road, Oxford OX1
3PT, UK and [2]Department of Neurobiology and the
Interdisciplinary Center for Neural Computation, Hebrew
University, Jerusalem, Israel

We characterized the functional organization of different fields
within the auditory cortex of anaesthetized ferrets. As previously
reported, the primary auditory cortex, A1, and the anterior auditory
field, AAF, are located on the middle ectosylvian gyrus. These areas
exhibited a similar tonotopic organization, with high frequencies
represented at the dorsal tip of the gyrus and low frequencies more
ventrally, but differed in that AAF neurons had shorter response
latencies than those in A1. On the basis of differences in frequency
selectivity, temporal response properties and thresholds, we
identified four more, previously undescribed fields. Two of these
are located on the posterior ectosylvian gyrus and were tonotopi-
cally organized. Neurons in these areas responded robustly to
tones, but had longer latencies, more sustained responses and
a higher incidence of non-monotonic rate-level functions than those
in the primary fields. Two further auditory fields, which were not
tonotopically organized, were found on the anterior ectosylvian
gyrus. Neurons in the more dorsal anterior area gave short-latency,
transient responses to tones and were generally broadly tuned with
a preference for high (>8 kHz) frequencies. Neurons in the other
anterior area were frequently unresponsive to tones, but often
responded vigorously to broadband noise. The presence of both
tonotopic and non-tonotopic auditory cortical fields indicates that
the organization of ferret auditory cortex is comparable to that seen
in other mammals.

Keywords: cortical field, ectosylvian gyrus, electrophysiology, frequency
tuning, non-primary, tonotopic

Introduction

Ferrets are increasingly being used for studying the functional
organization (Phillips *et al.*, 1988; Shamma *et al.*, 1993; Kelly and
Judge, 1994; Schnupp *et al.*, 2001; Innocenti *et al.*, 2002),
development (Chapman and Stryker, 1993; Juliano *et al.*, 1996;
Mrsic-Flogel *et al.*, 2003) and plasticity (Sur *et al.*, 1988;
Thompson *et al.*, 1993) of the sensory areas of the cerebral
cortex. Because of their particular suitability for behavioural
studies (Kavanagh and Kelly, 1987; King and Parsons, 1999;
Moore *et al.*, 1999), there is growing interest in the possibility of
using ferrets in chronic recording experiments, in order to
investigate the physiological changes underlying perception
and experience-driven plasticity (Fritz *et al.*, 2003).

In other mammalian species, including humans (Zatorre
et al., 2002), non-human primates (Merzenich and Brugge,
1973), cats (Woolsey *et al.*, 1960), guinea pigs (Redies *et al.*,
1989), gerbils (Thomas *et al.*, 1993) and rats (Sally and Kelly,
1988), auditory cortex has been divided into one or more
primary (or central 'core' areas in primates) and several non-
primary (or belt and para-belt) areas. Primary areas contain
neurons that typically respond with a short latency to pure

tones, exhibit a preference for a restricted range of frequencies
and display a clear tonotopic organization, with cells ordered
according to their preferred or 'best' frequency. In contrast,
neurons in non-primary areas can differ in their frequency
organization, response latencies, and spatial and spectral in-
tegration properties. Indeed, systematic variations in these
response properties have been used as a basis for segregating
different auditory fields into distinct processing streams (Rau-
schecker and Tian, 2000; Read *et al.*, 2002; Griffiths *et al.*, 2004).

Auditory cortex in the ferret occupies the ectosylvian gyrus
(EG), which has been divided, on the basis of the distribution of
sound-evoked 2-deoxyglucose activity, into three anatomically
distinct areas, one located on the middle ectosylvian gyrus
(MEG), another on the posterior ectosylvian gyrus (PEG) and
a third on the anterior ectosylvian gyrus (AEG) (Wallace *et al.*,
1997). This accords with the pattern of degeneration observed
in the auditory thalamus following EG lesions of differing size
(Kavanagh and Kelly, 1987). However, the response properties
of auditory cortical neurons in this species have yet to be
characterized in any detail. Electrophysiological studies have so
far been restricted to the MEG, where two tonotopically
organized fields have been described, the primary auditory
cortex, A1 (Kelly *et al.*, 1986; Phillips *et al.*, 1988), and the
anterior auditory field, AAF (Kowalski *et al.*, 1995). More
recently, however, optical imaging of intrinsic signals has
been used to confirm that areas on the PEG and the AEG are
also acoustically responsive and that they exhibit some degree
of frequency sensitivity (Nelken *et al.*, 2004).

The aim of the present study was to use multi-electrode
recording techniques to map the full extent of the ferret's EG.
By analysing frequency tuning parameters, tonotopic order and
temporal response properties of large numbers of units, we
have been able to subdivide the auditory cortex of this species
into at least six areas, four of which are previously uncharac-
terized, non-primary areas located on the AEG and PEG.

Materials and Methods

Animal Preparation
All animal procedures were approved by the local Ethical Review
Committee and performed under licence from the UK Home Office in
accordance with the Animal (Scientific Procedures) Act 1986. Five adult
pigmented female ferrets (*Mustela putorius*) were used in this study. All
animals had regular otoscopic examinations to ensure that both ears
were clean and disease free.

Anaesthesia was induced by 2 ml/kg i.m. injection of alphaxalone/
alphadolone acetate (Saffan; Schering-Plough Animal Health, Welwyn
Garden City, UK). The left radial vein was cannulated and a continuous
infusion (5 ml/h) of a mixture of medetomidine hydrochloride (0.022
mg/kg/h; Pfizer Ltd, Sandwich, UK) and ketamine (5 mg/kg/h; Fort
Dodge Animal Health, Southampton, UK) in physiological saline, which

was supplemented by 5% glucose, 0.5 mg/kg/h dexamethasone (Dexadreson; Intervet UK Ltd, Milton Keynes, UK) and 0.06 mg/kg/h atropine sulphate (C-Vet Veterinary Products, Leyland, UK) was maintained throughout the experiment. A tracheal cannula was implanted for artificial ventilation. The ventilator (Ugo Basile model 7025, Comerio, Italy) was placed outside the anechoic chamber in which the recordings were made, with air supplied to the animal via tubes that entered through a sealed hole in the chamber wall. Body temperature, inspired and expired CO_2 and electrocardiogram (ECG) measurements were carefully monitored to ensure stable and adequate anaesthesia.

The animal was placed in a stereotaxic frame and the temporal muscles of both sides were retracted to expose the dorsal and lateral parts of the skull. On the right side of the skull a metal bar was cemented and screwed in place, to hold the head without further need of a stereotaxic frame. On the left side, the temporal muscle was retracted and removed to gain access to the auditory cortex, which lies ventral to the suprasylvian sulcus (*sss*, Fig. 1) (Kelly *et al.*, 1986). Recordings were made from the left side of the brain only, to avoid the possibility of inter-areal or inter-animal differences resulting from any cortical asymmetries that may exist. The *sss* and the pseudosylvian sulcus (*pss*) were exposed by a craniotomy. The overlying dura was removed and the cortex covered with silicon oil. The animal was then transferred to a small table in an anechoic chamber (IAC Ltd, Winchester, UK).

Stimuli

Acoustic stimuli were generated using TDT system 3 hardware (Tucker-Davis Technologies, Alachua, FL). In two experiments (F0330, F0232), stimuli were presented via a closed-field electrostatic speaker (EC1, Tucker-Davis Technologies), whereas, in the other three experiments (F0313, F0321, F0333), a Panasonic headphone driver (RPHV297, Panasonic, Bracknell, UK) was used. The electrostatic drivers had a flat frequency output to 110 kHz, whereas the output of the Panasonic drivers extended to 30 kHz. Closed field calibrations were performed using an 1/8th inch microphone (Bruel and Kjær, Naerum, Denmark), placed at the end of a model ferret ear canal, to create an inverse filter that ensured the driver produced a flat (<±5 dB) output. All stimuli were presented contralaterally. Pure tone stimuli ranged, in 1/3-octave steps, from 500 Hz to 24 kHz (Panasonic driver) or 500 Hz to 30 kHz (TDT EC1 driver), and were 100 ms in duration (5 ms cosine ramped). Intensity levels were varied between 0 and 80 dB SPL in 10 dB increments. This totalled 150–200 frequency–level combinations, each of which was presented pseudorandomly, once per second, with typically three, and sometimes more, repetitions. Broadband Gaussian noise bursts, 40 Hz–30 kHz bandwidth and cosine ramped with a 10 ms rise/fall time, were generated afresh for each trial and used as a search stimulus. These noise bursts were varied in level from 30 to 80 dB SPL in 10 dB increments to establish whether each unit or unit cluster was acoustically responsive.

Data Acquisition

Silicon probe electrodes (16 channel, Universiy of Michigan) were used. In most recordings, we used probes with a 4×4 configuration, consisting of four electrodes, each with four active sites separated by a distance of
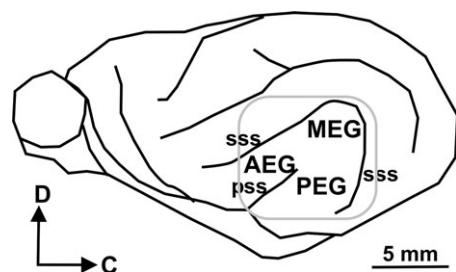

Figure 1. Schematic of the ferret's brain, showing the location of the ectosylvian gyrus (grey rectangle), which is subdivided into the middle ectosylvian gyrus (MEG), containing A1 and AAF, the posterior ectosylvian gyrus (PEG) and the anterior ectosylvian gyrus (AEG). Other abbreviations: *sss*, suprasylvian sulcus; *pss*, pseudosylvian sulcus,

200 μm. Typically, we were able to record on at least 12 of the active sites within any given penetration and recordings were often obtained at all 16 sites. In a small number of penetrations in one animal, we used a single probe with 16 active sites spanning a range of 1.6 mm along its length in order to sample responses at different cortical depths in more detail.

The neuronal recordings were bandpass filtered (500 Hz–5 kHz), amplified (up to ×20 000) and digitized at 25 kHz. Single units and small multi-unit clusters were isolated from the digitized signal. Data acquisition and stimulus generation were performed using BrainWare (Tucker-Davis Technologies). All subsequent analysis was performed using MATLAB (Mathworks, MathWorks, Inc.).

Data Analysis

Spike sorting was performed offline. Only signals with an amplitude three times that of the noise were recorded by the data acquisition software as 'spikes'. Units were isolated from the digitized signal by manually clustering data according to spike features, such as amplitude, width and area. We also inspected inter-spike-interval (ISI) histograms and only cases for which the ISI revealed a clear refractory period were classed as single units. For a minority of recordings, we were unable to demonstrate a refractory period and, in these cases, the unit was classified as a 'small cluster'. We saw no evidence for differences in the response properties or the cortical distribution of data from such clusters compared with those from single units and have not differentiated between them. The term 'unit' is therefore used to refer either to a single unit or a small cluster. Inclusion of small clusters in our analysis means that we might have missed some of the detailed differences in response properties between different cortical areas. However, our principal interest in this paper was to investigate the overall functional organization of a large area of cortex. Hence the inclusion of small clusters will tend to make us more conservative in assigning differences between the fields. We also carefully examined the spike shapes and ISI histograms for units recorded on neighbouring probe sites to ensure that responses on each recording site represented independent units.

All data presented are from units whose spike counts following the stimulus were significantly different from the spike counts in windows of the same duration just preceding stimulus onset ($P < 0.05$, paired t-test on all stimulus presentations). For the tonal stimuli, this is a conservative test, since some of the stimuli [those outside the frequency-response area (FRA)] were ineffective. The test was done for both noise stimuli and for the tonal stimuli, and units were included when they showed a significant response to either the tone or to the noise stimuli. All units considered in the quantitative analysis of response parameters produced a significant response to tone stimuli.

FRAs were constructed for all recordings by summing activity that occurred during a response window (usually 200 ms) for all repetitions of each frequency–level combination. This spike matrix was smoothed with a nine-point running hamming window. This smoothing window has an equivalent rectangular area of four bins, and is therefore roughly equivalent to the use of a square smoothing window with an edge of two bins. Units were deemed to have responded to frequency-level combinations that elicited more spikes than a criterion level, which was defined as the mean spontaneous rate plus 20% of the peak firing rate (Sutter and Schreiner, 1991). This criterion level was used to construct a tuning curve, from which other parameters (such as characteristic frequency, CF, and tuning properties, see below) were extracted. This algorithm was performed automatically by MATLAB. All FRAs were individually examined and, in the vast majority of cases, this algorithm produced results that corresponded to those determined by visual inspection.

CF was defined as the frequency that elicited a response at the lowest sound level. Where more than one frequency was effective at threshold, the logarithmically weighted mean was used. For plotting these values over the cortical surface, the characteristics of each penetration were assigned to those points that were nearer to it than to any other penetration using Voronoi tessellation (MATLAB, MathWorks, Inc.). All units with a bandwidth of less than two octaves at 10 dB above threshold were, for the purposes of displaying the representation of sound frequency over the surface of the cortex, assigned a single CF. Units with Q10 values (CF divided by the frequency range that evoked

a significant response at 10 dB above threshold) greater than this were deemed to be untuned.

Minimum response latencies were computed as the time at which the pooled response first crossed a critical level defined as 20% of the difference between the spontaneous and peak firing rates. Latency measures were extracted from a pooled post-stimulus time histogram (PSTH) containing the responses to all frequency–level combinations. Response duration was calculated as the difference between the timing of the first evoked spike and the latest time that the spike rate exceeded this critical value. Peak response latencies were defined as the time at which the maximum spike rate occurred.

Results

We present here the data from a total of 1972 recording sites in five animals. Between 246 and 570 units were recorded in each of these animals. Table 1 summarizes the total number of units recorded in each animal. About two-thirds of the units (1202/1972) responded to both tones and noise. However, there were significant populations that responded either to tones only (564/1972) or to noise only (128/1972). As shown later, neurons that responded to noise only occurred mostly in non-primary areas.

Frequency Response Areas

Most units exhibited onset responses to pure tones. These responses were frequently accompanied by more sustained discharges, which in many cases occurred well after stimulus offset. Examples of the PSTHs encountered are shown in Figure 2. As previously reported, for example, in the cat posterior auditory field, PAF (Loftus and Sutter, 2001), FRAs constructed from the initial and later components of the response occasionally differed, with more complex responses associated with later spikes. However, the later response almost invariably had a higher threshold than the onset component and therefore inclusion of both within the response period did not usually affect the derived CF. Indeed, comparison of the CF values derived for different response windows revealed very little change in tuning, with only 14% of units exhibiting a shift in CF of >0.5 octave when the response window was increased from 100 to 200 ms after stimulus onset. Units whose CF did change in this fashion were scattered throughout the EG. Twenty per cent of the units continued to respond beyond 200 ms after stimulus onset, with 10% responding after 250 ms, but extending the response window for these units had a negligible effect on the overall distribution of CFs. Because we were primarily interested in comparing the responses of units in different cortical areas and wanted to apply the same analysis to each one, FRAs were constructed for all units using the first 200 ms after stimulus onset. From the resulting tuning curves (denoted by the white lines in the examples shown in Figure 3; see Materials and Methods for details of how these were calculated), we extracted the CF, Q10 and Q30.

Table 1
Number of acoustically responsive neurons recorded in the auditory cortex of each animal

Animal	Total number of units	Grand totals	n
F0313	366	Total number of units	1972
F0321	246	Number of tone-responsive units	1834
F0330	506	Number of noise-responsive units	1352
F0333	284	Units responding to both	62%
F0232	570		

Cortical Representation of Sound Frequency

Figure 4 shows the CF tessellation maps for each of the five animals. Recording sites located down a sulcus have been unfolded to produce a two-dimensional representation of sound frequency. We were able to assign a CF for the majority of units, as indicated by the coloured polygons. Light grey polygons represent units classified as 'untuned' and dark grey polygons indicate units that did not respond to pure tones but did respond to broadband noise.

Middle Ectosylvian Gyrus

The frequency organization of the primary areas, A1 and AAF, on the MEG varied somewhat between animals, although a dorso-ventral progression from high to low frequencies was apparent in each case (Fig. 4). The distribution of sampling sites was sometimes limited by the vasculature of the cortex in that, in several animals, there were regions (such as the anterior edge and the mid-frequency portion of the MEG) where the presence of blood vessels prevented us from inserting the silicon probe electrodes. Within the region of MEG sampled, we were typically unable to identify separate dorsoventrally oriented frequency gradients that would correspond to these two tonotopic areas. However, in one animal (F0330, Fig. 4A), two foci of high-frequency selectivity at the apex of the MEG appeared to be separated by a region with tuning to lower frequencies (orange polygons near the tip of the MEG). It has been reported (Kowalski et al., 1995) that the frequency
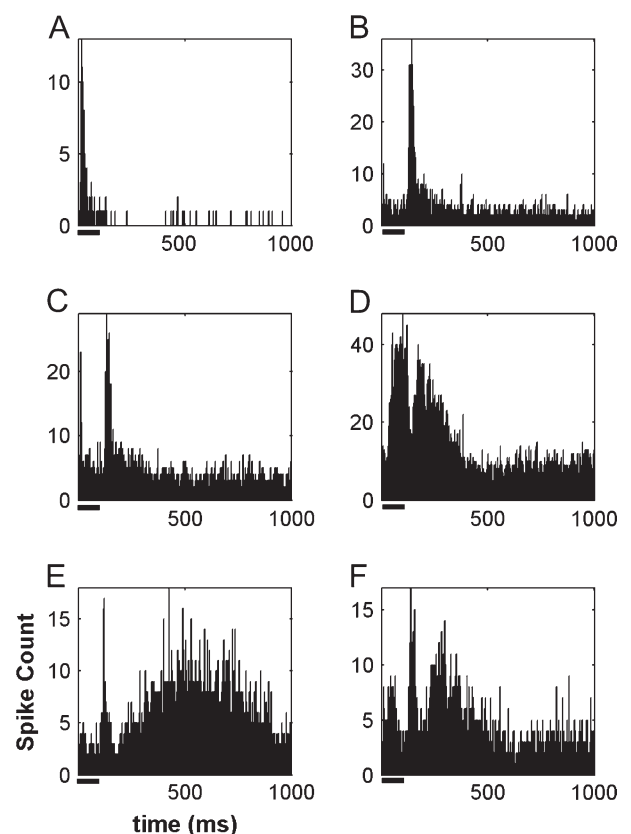

Figure 2. Examples of PSTHs recorded in response to pure tone stimuli for six different cortical neurons. These were selected to illustrate the range of temporal firing patterns encountered. Bars underneath the x-axes indicate the stimulus duration. Spike counts per bin (1 ms) were summed across three stimulus repetitions.
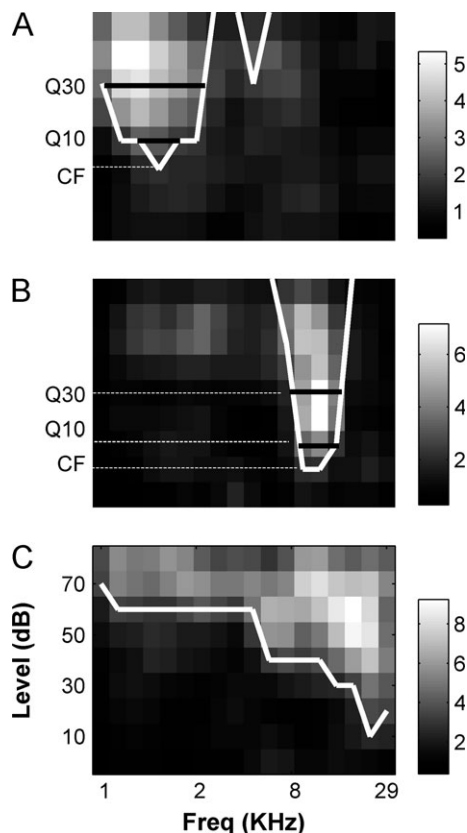
Figure 3. (*A–C*) Three examples of frequency-response areas, illustrating a range of characteristic frequencies (CF) and tuning bandwidth. The white line in each case delineates the 'tuning curve' (see Materials and Methods), from which the CF, Q10 and Q30 values were calculated. The grayscale squares indicate the number of spikes evoked at each frequency–level combination.

gradient in AAF runs rostroventrally, with its low-frequency representation lying within the sss. In two animals we recorded units within the sss. In one case (F0333, Fig. 4*D*), there was a progression in CF to lower frequencies with increasing depth into the sulcus. However, in animal F0232 (Fig. 4*B*), more extensive recordings failed to show any evidence of a progression, with units recorded over >2.5 mm having high-frequency CFs. Therefore it appears that the exact orientation of the anterior field, like A1, varies between animals.

Posterior and Anterior Ectosylvian Gyri

An area of low-frequency sensitivity was present on the PEG, which was continuous with the low-frequency area on the ventral region of the MEG (Fig. 4*A–C,E*). This low-frequency tuned area formed a narrow strip running dorsoventrally and subdivided two regions of high-frequency selectivity, located at the anterior and posterior extremes of the ventral PEG. This is most apparent in Figure 4*A–C*. Examination of responses recorded in this area revealed that most had clear frequency tuning, with an unambiguous CF. However, units located at the most ventral extremes and very close to the *sss* were more broadly tuned, often having weak tone responses and fragmented FRAs.

The distribution of CFs suggested that the acoustically responsive area of the AEG might also be subdivided into different regions. At the most ventral extreme, units were only weakly responsive to tones and 19% were untuned or exhibited

broad tuning. Moreover, 14% of the units found in this region of cortex responded to broadband noise but not to tones (clustering of dark grey polygons in Fig. 4*A,B,E*). In contrast, a CF could be assigned to >80% of units located between this ventral area and the low-frequency representation of A1 in the MEG, and the majority of these were broadly tuned to high frequencies (e.g. >8 kHz). However, there was little evidence of any tonotopic progression; rather, we observed a rapid transition from low CF to high CF units (Fig. 4*A,D*).

Frequency reversals and the presence of regions where there is a transition from tuned to untuned units are indicative of boundaries between neighbouring auditory fields. For example, on the PEG we observed two areas of high-frequency sensitivity, which are separated from A1, and from each other, by regions of low-frequency tuning. At least three potential groupings of neurons in this part of auditory cortex could exist. Firstly, these two areas could share the low-frequency representation that runs dorsoventrally through the PEG, and therefore have opposing frequency gradients that are oriented rostrocaudally. Secondly, the low-frequency area could be continuous with the more posterior high-frequency region only, forming a single caudal-to-rostral, high-to-low tonotopic map, while the more anterior high-frequency region shares a low-frequency border with A1, thereby having a ventral-to-dorsal, high-to-low organization. The third possibility is that the more posterior field on the PEG shares a low-frequency border with A1, whereas the low-frequency region in the middle of this gyrus constitutes part of the more anterior area.

In order to help us distinguish these possibilities, we examined FRAs along vectors across the cortical surface (Figs 5 and 6). In moving dorsoventrally across the posterior part of the MEG in animal F0330 (along the arrow in Fig. 5*A*), we observed discrete FRAs and a systematic decrease in CF (Fig. 5*B*, units a–k). However, FRAs from units located at the transition between MEG and PEG (units l and m, marked with asterisks) were fragmented, beyond which the FRAs became clearer again and their CFs increased (units n–t). This sequence indicates the presence of a dorsoventrally oriented frequency gradient within the anterior part of the PEG. Two other examples of how the FRAs change across the cortical surface are shown for animal F0232 in Figure 6. The dorsoventral sequence across the anterior part of the EG (solid arrow in Fig. 6*A*) again revealed a systematic decrease in CF (Fig. 6*B*, units a–i). At more ventral locations, however, the FRAs were broader and, in most cases, dominated by high frequencies (Fig. 6*B*, units j–o). The caudorostral vector through the PEG (dashed arrow in Fig. 6*A*) confirmed the presence of a high–low–high sequence of frequency sensitivity (Fig. 6*C*, units p–y). Moreover, because a smooth progression in CF was found from the more posterior high-frequency area to the low-frequency strip in the middle of the PEG (units p–u), we grouped these regions into one field and, in keeping with the second possibility mentioned above, assigned a second cortical field to the dorsoventral frequency gradient on the anterior aspect of the PEG.

Subdivision of Auditory Cortex

On the basis of the CF maps produced for each animal (Fig. 4) and the variation in FRAs plotted along vectors across the cortical surface (as in Figs 5 and 6), we subdivided the EG into six areas. These are shown schematically in Figure 7 and are indicated by the dashed lines in Figure 4. We have adopted a nomenclature based on anatomical landmarks for the fields
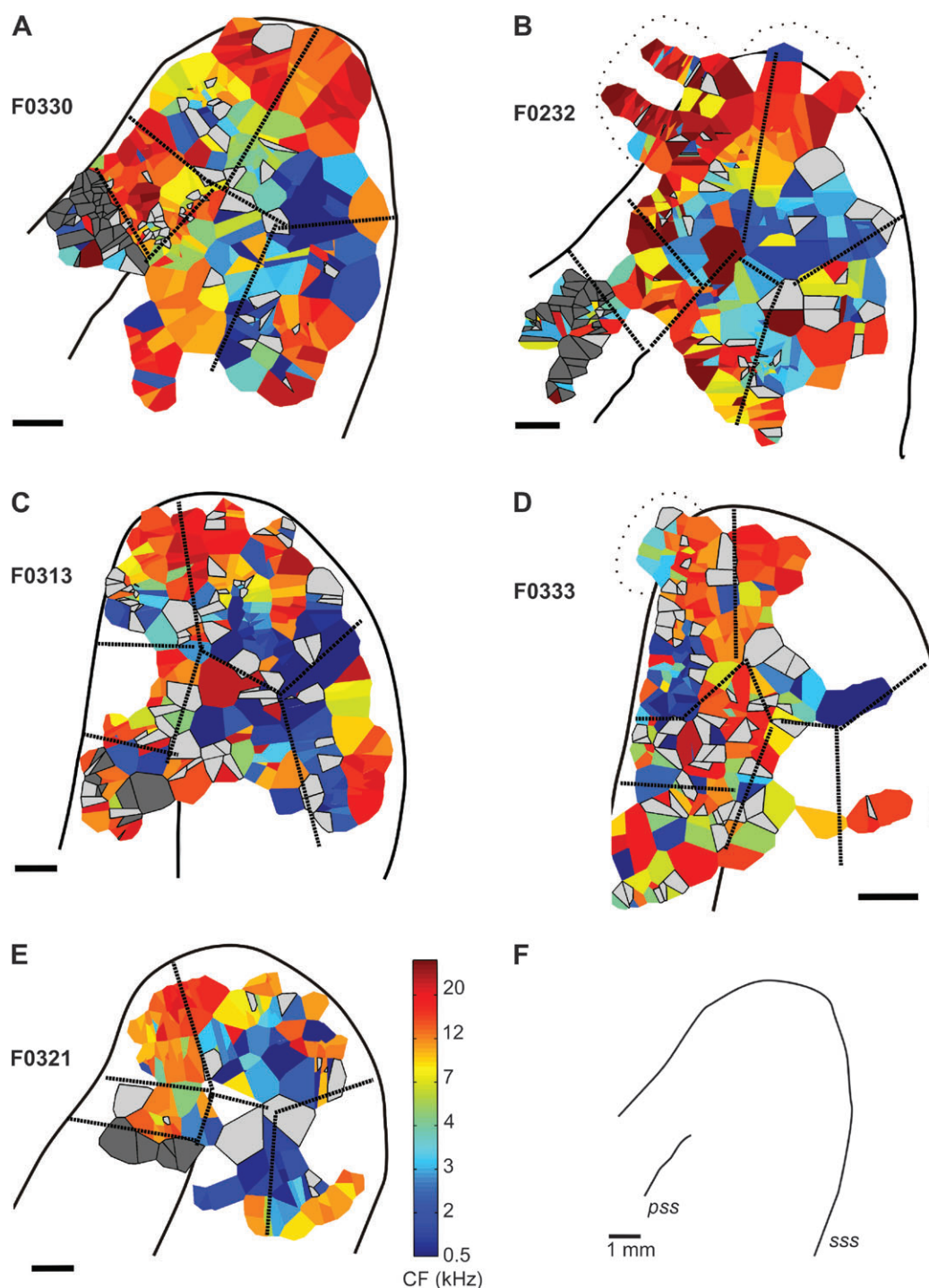
Figure 4. (*A–E*) Voronoi tessellation maps illustrating the frequency organization of the auditory cortex in all five animals used in this study. Coloured polygons indicate cortical locations where a characteristic frequency was assigned. Grey polygons indicate that the unit was either untuned (light grey) or responsive only to noise stimulation (dark grey). (*B*, *D*) Some recordings were made from the anterior or dorsal banks of the suprasylvian sulcus (*sss*), which have been unfolded in order to produce a two-dimensional representation of characteristic frequency. (*F*) Schematic of the ectosylvian gyrus. Dashed lines indicate prospective field boundaries made on the basis of both the distribution of frequency tuning and differences in unit response properties. Other abbreviation: *pss*, pseudosylvian sulcus. Scale bars indicate 1 mm.

that have not previously been described, rather than terms that are commonly used in other species, because we do not wish to imply that they are necessarily homologous to specific areas that have been described in detail in those species. A quantitative analysis of both the CFs and other response properties is presented in the following sections, which shows significant inter-areal differences in their distribution across the auditory cortex.

In keeping with previous studies, we recognize two primary auditory fields located on MEG, A1 and AAF. Although the dorsal high-frequency region of the MEG usually lacked an obvious border between these fields (with the possible exception of
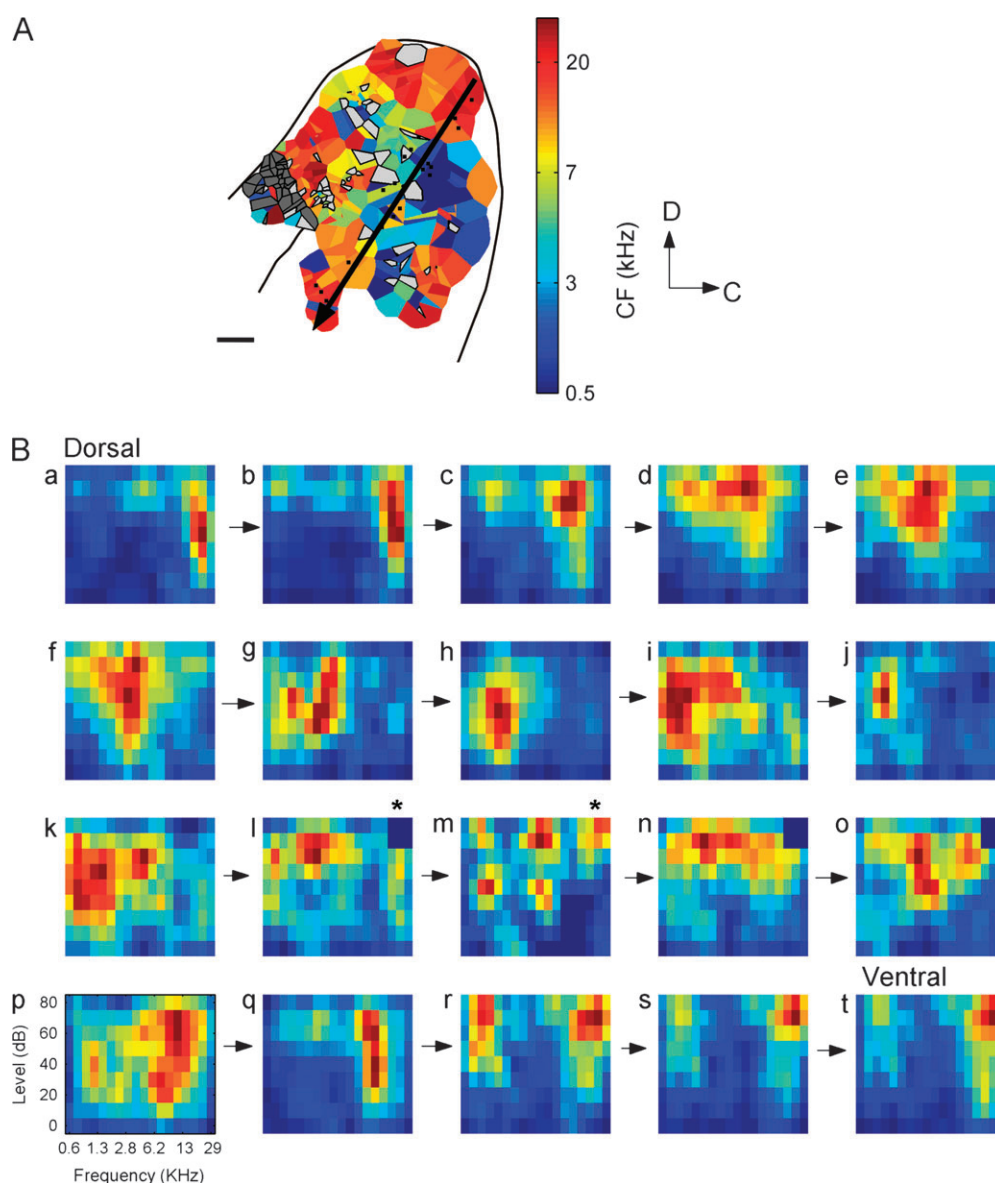
Figure 5. Variation in characteristic frequency across the cortex. (*A*) Voronoi tessellation map illustrating the frequency organization of the auditory cortex of animal F0330. (*B*) Examples of frequency-response areas plotted along a vector running dorsoventrally across the posterior part of the EG (black arrow in *A*). Note the shift in tuning from high to low frequencies for units a–k, followed by the more fragmented frequency-response areas of units l and m (asterisks), and then another systematic progression from low to high frequency tuning (units n-t).

F0330, Fig. 4*A*), the dorsoventral frequency gradients were (to varying extents) oriented caudally in the case of A1 and rostrally in the case of AAF (this is most obvious in Fig. 4*A,C*).

Using the same criteria, the PEG was also divided into two areas. The more anterior region, with its dorsoventral frequency gradient (Fig. 5), is bordered by the *pss* rostrally and A1 dorsally, while the more posterior region, with its rostrocaudal gradient (Fig. 6), is bordered by the *sss* and again by A1 dorsally. For the purpose of further analysis, these have been designated the posterior pseudosylvian field (PPF) and the posterior suprasylvian field (PSF), respectively.

AEG was also subdivided into two areas. The more dorsal area (anterior dorsal field, ADF) is bordered by the *sss* rostrally, AAF dorsally and PPF caudally, and contains tuned neurons with high CFs. Ventral to this, the anterior ventral field (AVF) consists of the group of neurons that generally did not respond well to tones and showed little frequency tuning.

Inter-areal Differences in the Representation of Sound Frequency

These sub-divisions were then used as a basis for further analysis of cortical response properties, both within and between the different areas. Figure 8 shows representative FRAs from one penetration in each area. The FRAs are arranged according to which of the 4×4 array of recording sites on the silicon probe they were obtained from. An empty space indicates that no response was recorded at that site. In the examples shown, responses to tones could be recorded at most sites in five out of the six areas (Fig. 8*A*–*E*), whereas only 7/16 sites in area AVF elicited a response to tones (Fig. 8*F*), with one further site responding to noise only (empty box). A patchy distribution of acoustically responsive neurons was characteristic of all our recordings in AVF.

Units in A1 (Fig. 8*A*) and in AAF (Fig. 8*B*) usually had sharply tuned, V-shaped FRAs. Units recorded in the two PEG areas (PPF
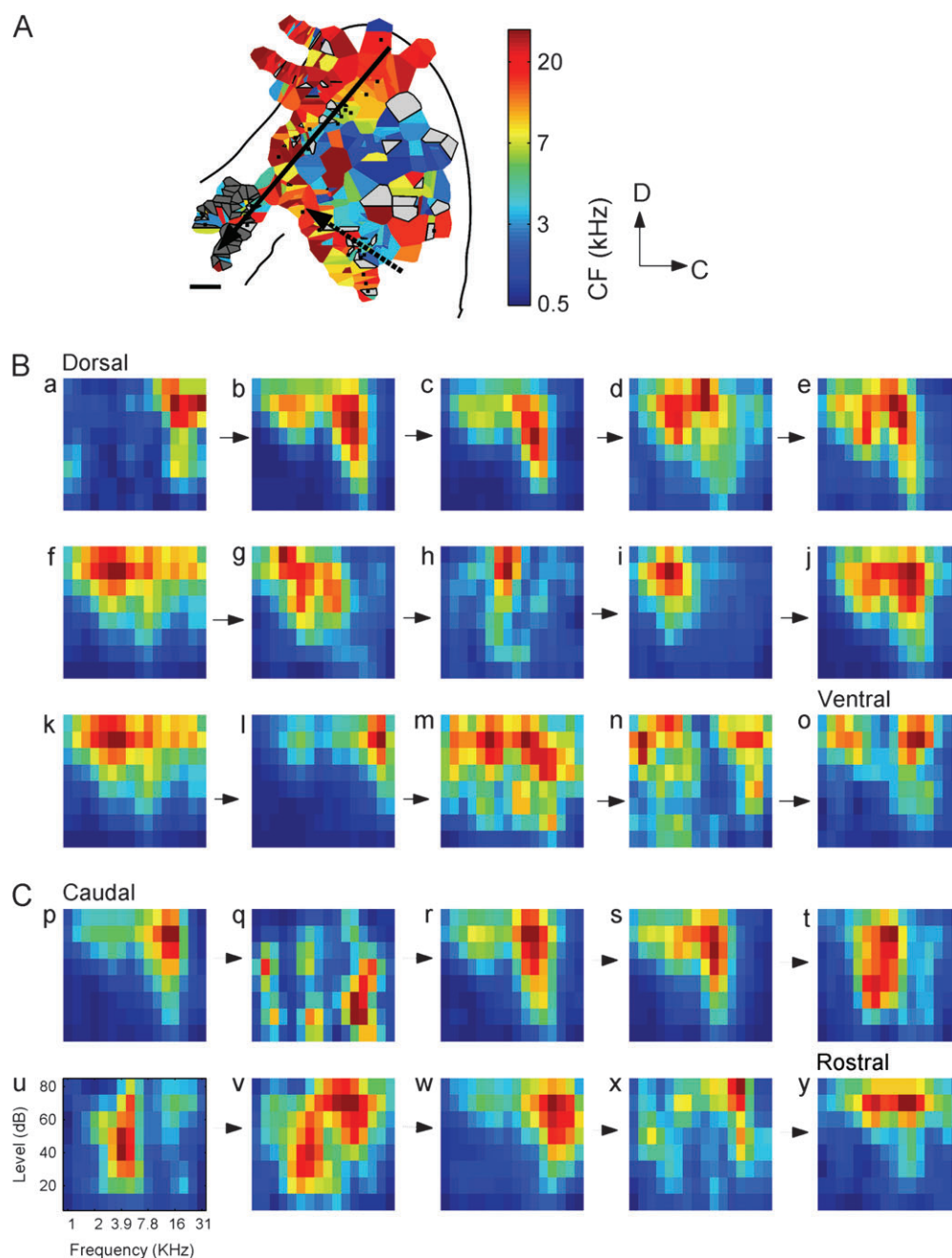
Figure 6. Variation in characteristic frequency across the cortex. (A) Voronoi tessellation map illustrating the frequency organization of the auditory cortex of animal F0232. (B) Examples of frequency-response areas plotted along a vector running dorsoventrally across the anterior part of the EG (solid arrow in A). Note the systematic decrease in frequency tuning for units a–i, followed by units with broader frequency-response areas (units j–o). (C) Examples of frequency-response areas plotted along a vector running caudorostrally across the PEG (dashed arrow in A). In this case, the tuning shifts gradually from high to low frequencies and then increases again.

and PSF) also displayed clear frequency tuning and a particular tendency toward non-monotonic response-level functions, indicating a preference for particular frequency–level combinations (Fig. 8C,D). As in other studies (Kitzes and Hollrigel, 1996), these functions were classified as non-monotonic if the response at CF (±one frequency bin) fell to <50% at a sound level above that where the maximum firing rate was obtained. A comparison of the proportions of non-monotonic units over the MEG and PEG revealed that these were not uniformly distributed ($\chi^2 = 6.836$, df = 1, $P < 0.01$). As expected, we found more non-monotonic units in the posterior fields (25% and 20% for

PPF and PSF, respectively) than in the MEG (16% for A1 and 17% for AAF, respectively). Compared to AVF (Fig. 8F), units in ADF (Fig. 8E), the other field on the AEG, gave robust responses to tones, but were broadly tuned with a preference for high frequencies.

As Figure 8 shows, CFs from adjacent positions on the electrode were often very similar, although we observed a difference of 0.90 octaves on average between the bottom and top recording site. This suggests that laminar differences in CF exist, particularly in the AEG. However, although we attempted to position the recording probe approximately
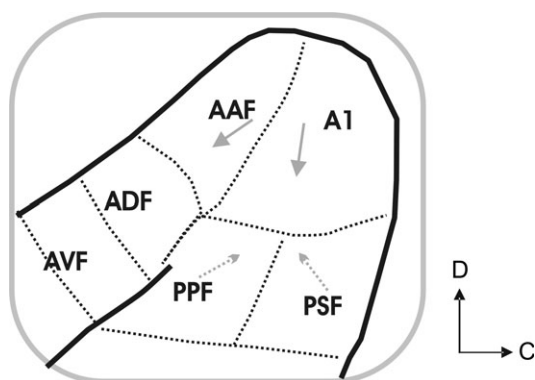
Figure 7. Schematic of the six auditory areas described here. The grey arrows indicate the order (from high to low) in the tonotopic representations. A1, primary auditory cortex; AAF, anterior auditory field; ADF, anterior dorsal field; AVF, anterior ventral field; PPF, posterior pseudosylvian field; PSF, posterior suprasylvian field.

orthogonal to the surface of the cortex, because of differences in curvature, this was not always precisely the case. Some of the observed changes in CF with depth may therefore reflect differences in the relative intralaminar locations of the recording electrodes.

The frequency representation in each of the fields was examined quantitatively by plotting cumulative polygon areas for CF in each animal (Fig. 9). If the CFs are represented evenly within a cortical field the cumulative area curve should have an approximately constant gradient. If there is an under-representation of a certain frequency the local slope will be shallower for that frequency range. Within A1 the gradient is reasonably constant (Fig. 9A), apart from one case (F0333, represented by the diamonds), where this region of cortex was relatively poorly sampled. AAF by comparison appears to under represent the middle frequencies in all animals (Fig. 9B). Although this is consistent with studies of AAF in the cat (Imaizumi *et al.*, 2004), it should be noted that, in three of our animals, the location of blood vessels prevented us from sampling the *sss*, where low-frequency AAF could be located (Kowalski *et al.*, 1995). Compared with A1, one of the posterior fields, PPF, under represents low sound frequencies (Fig. 9C). By contrast, area PSF is dominated by both low and high CF units, with very few units tuned to intermediate values (Fig. 9D), although the precise location of the boundary placed between the two posterior fields obviously determines the extent of the difference in the low-frequency representation between them. The initial shallow slope of the cumulative area curves for ADF indicates a clear under-representation of low frequencies (Fig. 9E), while AVF had a more variable pattern, consistent with the paucity of units that exhibited significant frequency tuning (Fig. 9F).

We further examined the distribution of CFs across the cortex by quantifying the degree of clustering using an objective method developed by Nelken and Versnel (2000) and refined by Rotman *et al.* (2001). All pairs of recordings were divided into 10 increasing subsets, with each subset including pairs separated by increasingly larger topographic distances. The CF differences for all pairs of units in each of these sets were computed and the 80th percentile was taken as a representative parameter difference for this set. The 80th percentile was chosen because although for a small cortical distance we might expect small differences in CF, some of the measured differences may still be large if, for example, a pair is positioned across a cluster boundary. This analysis resulted in a set of

typical CF differences as a function of topographic distance between recording sites. For parameters that cluster topographically, it is expected that these typical differences will increase as a function of distance. To determine significance levels, results of 1000 random permutations of CF across recording locations were used to compute the 10th and 90th percentiles of the typical differences (Figs 10 and 11). Values falling within this range indicated an absence of clustering.

The tendency for CF to cluster was tested both across the entire cortex for different animals and within the putative areas defined above for individual animals. Figure 10 shows the clustering of CF across the entire EG for each of five animals. In all cases, we observed an increase in mean CF difference as cortical distance was increased, with CF differences at small separations between recording locations falling outside the confidence limits in each case. Figure 11 shows the same analysis applied to one of these animals (F0232) for each of the six cortical fields. As expected, a progressive increase in CF difference with increasing cortical distance was apparent for the primary fields, A1 and AAF (Fig. 11A,B). The change in CF with cortical distance fell below the 10th percentile at all distances, indicating significant clustering in the representation of sound frequency. Significant clustering of CF was also seen in fields PPF and PSF (Fig. 11C,D), although both clusters were smaller than in the primary fields. The smaller cluster size may be due to less precise topography or, alternatively, to the smaller size of these fields. Finally, the fields that we have already described on the AEG as lacking tonotopic order essentially failed to show any significant clustering of CF (Fig. 11E,F). Although consistent with the segregation of cortical response properties into different fields, it should be stressed that the tendency to cluster shown by this method does not indicate how those responses are arranged within each field. Nevertheless, the other analyses described above reveal systematic order in the representation of CF within the primary fields and to a lesser extent on the PEG.

Representation of Other Response Parameters
In addition to the CF, where present, we derived each unit's response threshold, Q10 and Q30, the minimum response latency, peak response latency and response duration. All of these response measures were plotted across the surface of the cortex to produce tessellation maps for each response parameter (shown for Q30, minimum response and peak latency, and for threshold in Fig. 12). The results of a quantitative comparison between the response parameter values recorded in different cortical fields are provided in Figure 13. Tests for normality revealed the data to have a non-normal distribution. and so a non-parametric analysis of variance (Kruskal–Wallis test) was used. Because a significant effect of cortical area on each of the response parameters was observed, post-hoc pairwise comparisons (Tukey's honest significant difference test) were performed. Significant differences between individual areas are shown by the black lines above the plots.

Frequency Tuning
No obvious pattern was apparent in the distribution of Q30 values (Fig. 12A), although subsequent analysis revealed that the highest Q10 (Fig. 13A) and Q30 (Fig. 13B) values were found in the primary areas, A1 and AAF, and in area PPF. No significant differences were found between these areas. Because Kowalski
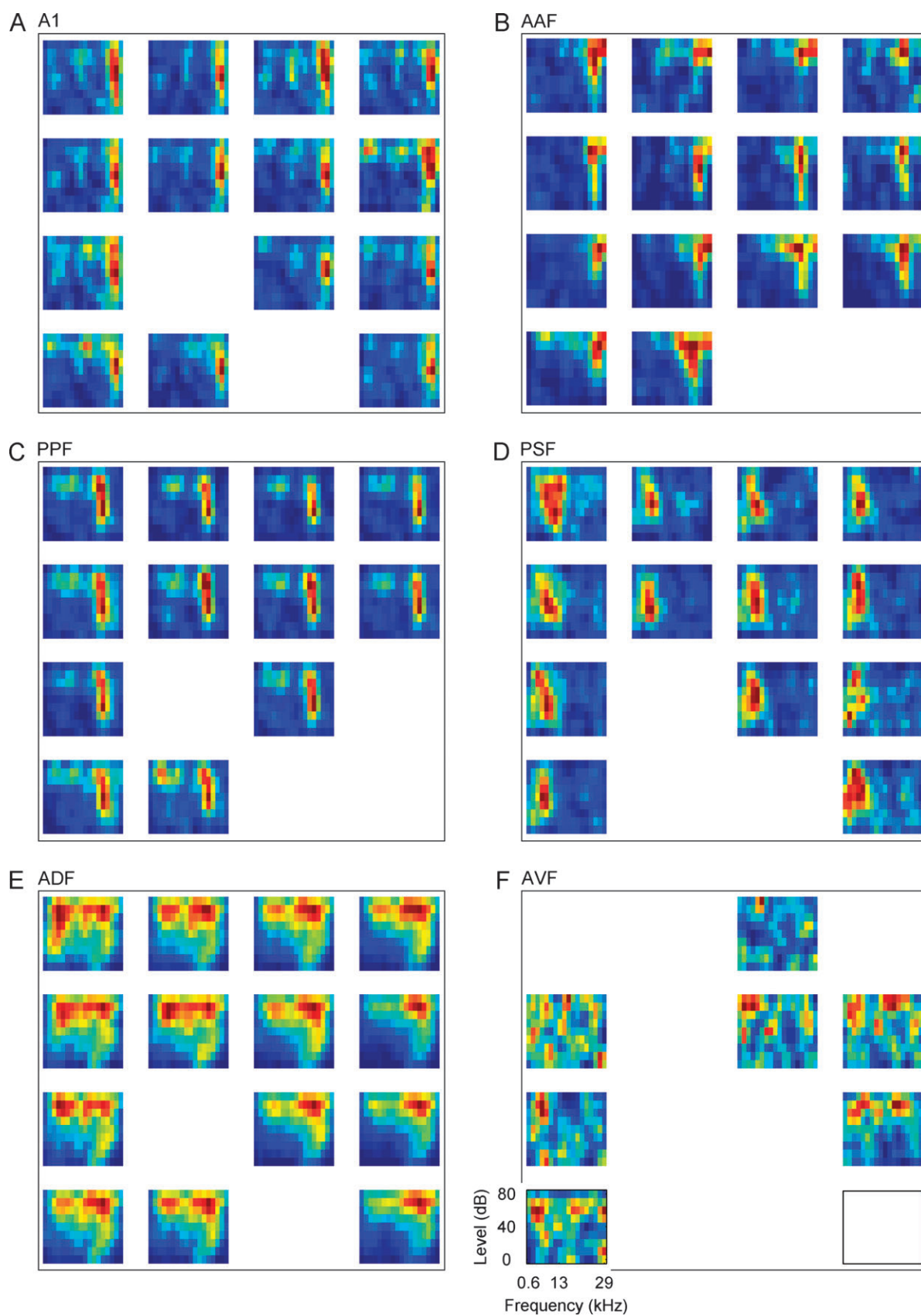
Figure 8. (*A-F*) Examples of frequency-response areas recorded with a silicon probe electrode with a 4×4 arrangement of recording sites from the six different areas of cortex. An empty space indicates that there was no response recorded at that site, while the empty square in *F* represents a unit that responded to broadband noise but not to tones.
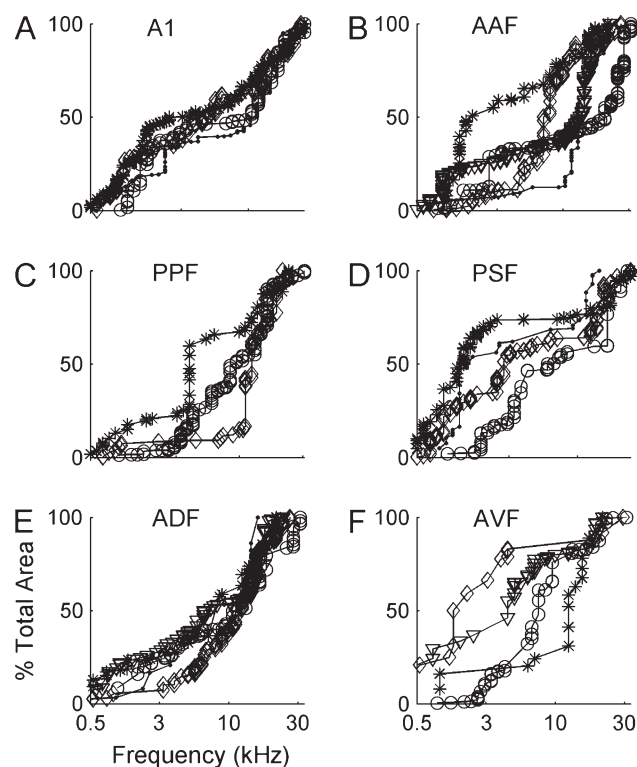
Figure 9. (*A–F*) Cumulative area distributions showing the representation of characteristic frequency in each of the six cortical fields. Each line represents the data from a different animal. A constant gradient indicates a uniform representation of sound frequency.

Figure 10. Clustering of unit characteristic frequency within the auditory cortex. (*A–E*) Cluster sizes in each of the 5 animals. Data have been pooled across all 6 cortical fields. The 10th and 90th percentiles (dotted lines) and the median (dashed line) of bootstrapped values from data randomly distributed among different electrode penetrations (see text) are shown. The actual values are shown by the solid black lines. Values that fall outside the confidence limits are considered significant. The cluster size is taken as the cortical distance travelled before these values cross the 10th percentile (lower dotted line).

et al. (1995) have reported that ferret AAF units are more broadly tuned than those in A1, we also compared the Q10 and Q30 values of AAF units recorded from within the anterior *sss* with those recorded in the rest of this field. However, we found no difference in tuning between these regions (not shown), suggesting that the difference between our results and those of Kowalski *et al.* (1995) is not a result of sampling differences. As expected from the example FRAs presented in Figure 8, the tuning of units recorded in the anterior fields (ADF and AVF) was much poorer. The analysis presented here underestimates the differences between the anterior fields and the other fields, because it is based only on units that gave significant responses to tones. Many AVF units could not be driven by tones or have CFs assigned, and were therefore not included when making these comparisons.

Threshold

Unit threshold measurements also differentiated between the auditory areas on the MEG and PEG, on the one hand, and those on the AEG on the other (Figs 12*D* and 13*F*). ADF and AVF units had significantly higher thresholds than in any of the other areas.

Temporal Response Properties

Examination of temporal response properties (Figs 12*B* and 13*C* for minimum response latencies, and Figs 12*C* and 13*D* for peak response latencies) shows that, in general, units recorded in the MEG and AEG had shorter latencies than those located in the PEG. We analysed the temporal response properties within each
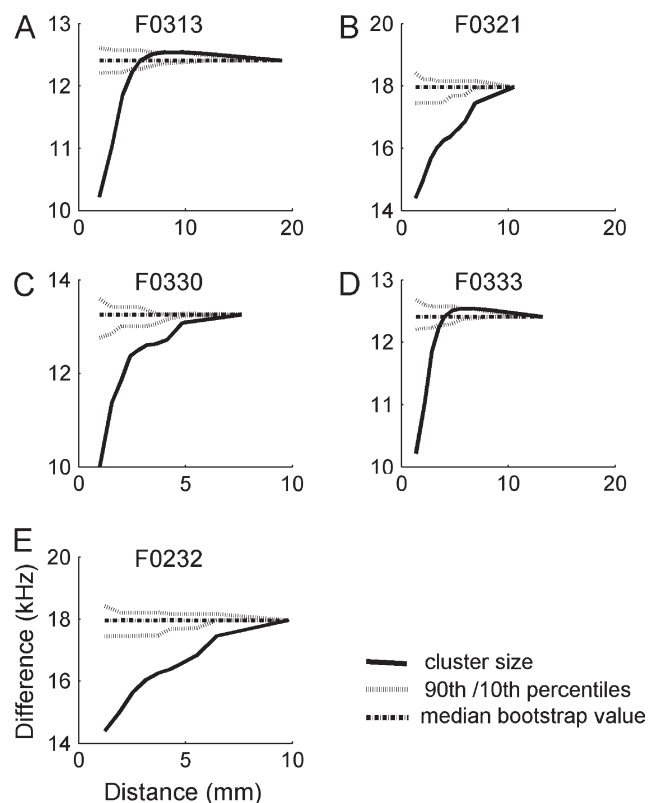
field, initially within individual animals, and, once we had confirmed that the trends were consistent, data were pooled across all animals. We created grand average PSTHs for each area by summing the normalized PSTHs from all units within that area. Figure 14 illustrates these grand average PSTHs for all five animals (black lines), together with those from one representative individual (shown in grey).

The pooled PSTHs for the primary fields exhibited two peaks, an onset response and a second response occurring just after stimulus offset, presumably representing an offset response (Fig. 14*A,B*). AAF units had the shortest minimum response and peak latency and both were significantly shorter than those recorded in A1 (Fig. 13*C,D*). On the other hand, neurons in the posterior areas responded with significantly longer response latencies (Fig. 13*C,D*) and tended to show more sustained firing patterns (Fig. 13*E*), with single units frequently having multi-peaked PSTHs (Fig. 14*C,D*). This contrasted with units recorded in the anterior areas, which generally had a single peaked onset response (Fig. 14*E,F*). Their latencies were also shorter than those in both posterior fields (Fig. 13*C,D*).

These observations were further quantified by comparing three sets of (dis)similarity measures between the pooled PSTHs of 1834 pairs of units, quantified as the sum of squares of the differences between pairs of PSTHs. In the first set, the dissimilarity between all possible pairs of PSTHs from different animals and different areas were computed. In the second set,
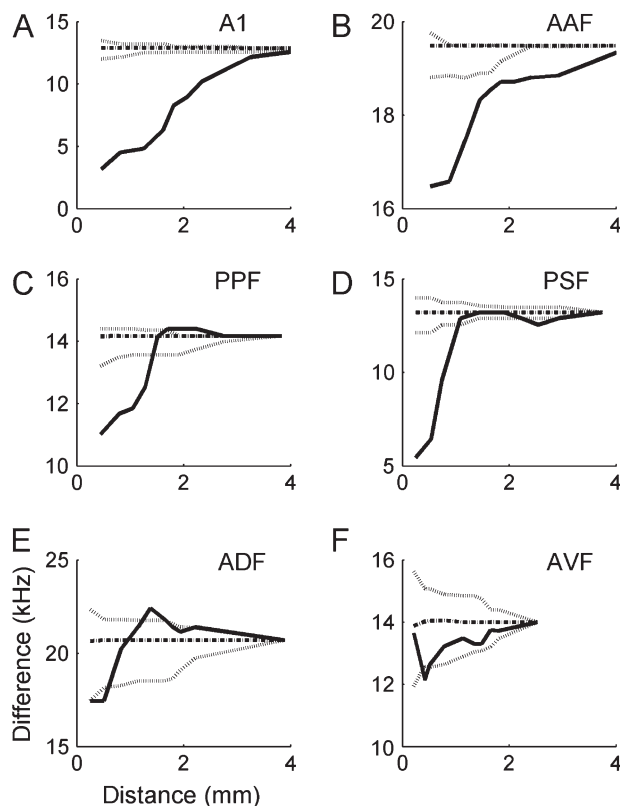
Figure 11. Clustering of unit characteristic frequency within the six different fields of the auditory cortex in one ferret. Other details as in Figure 10. Note that significant clustering of characteristic frequency was observed for the primary fields, A1 (*A*) and AAF (*B*), and to a lesser degree for the posterior fields, PPF (*C*) and PSF (*D*), but only to an extremely limited extent for the anterior fields, AVF (*E*) and ADF (*F*).

the dissimilarity between the PSTHs from the same area but from different animals was calculated. Finally, the third set consisted of the dissimilarity between PSTH pairs from different areas within single animals. We would expect that the largest dissimilarities should be observed in the set of all PSTH combinations. Moreover, if there are real inter-areal differences between the PSTHs that are consistent across animals, then the dissimilarities should be greater for comparisons of PSTHs from different areas within each animal than for comparisons of PSTHs from the same area across different animals. This pattern of results was observed [$F(2,403) = 4.64$, $P < 0.010$], with the dissimilarities being greatest in the across-area/across-animal comparison and smallest in the within-area/across-animal comparison. The across-area/within-animal value lay between these two. Post-hoc comparisons revealed that the within-area/across-animal sum of differences was significantly smaller than the across-area/across-animal comparison (Tukey's honest significant difference test, $P < 0.05$).

Cluster analyses were also performed for minimum response latencies, peak latencies, response duration, Q10 and Q30 values (see Table 2). For each area in each animal, the maximum distance at which the cluster values were still below the 10th percentile bootstrap values was extracted. Table 2 shows the across-animal median (with inter-decile ranges) of these values for each response parameter, including CF. Comparison of the medians reveals that the largest cluster sizes were obtained for CF than for other response measures, although this was the case

only in the primary areas, A1 and AAF. In most cases, the cluster sizes obtained for temporal response properties and frequency tuning were very small, especially within the anterior fields, indicating that clustering occurred at a very local level only. In all fields, at least two of the temporal parameters (response duration, minimum response latency and peak latency) showed a larger cluster size than the bandwidth parameters, Q10 and Q30. Indeed, the median values indicate that no clustering was apparent for Q30 in any of the cortical areas. Examination of the auditory cortex as a whole revealed larger cluster sizes than within individual areas; this is to be expected because of the larger area examined. However, the ordering of the cluster sizes in the global analysis was somewhat different, with clusters of Q30 being larger than expected based on their within-area cluster size. This suggests that Q30 clusters delimit areas, but the within-area distribution of Q30 is not clustered.

Discussion

Our electrophysiological recordings have confirmed the results of previous 2-deoxyglucose (Wallace *et al.*, 1997) and optical imaging (Nelken *et al.*, 2004) studies, by showing that acoustically responsive neurons are found within a large expanse of the ferret EG. By analysing the spectral and temporal response properties of these neurons, we have been able to divide the EG into six separate acoustically responsive areas. Neurons located in these areas differ in terms of their frequency tuning, range of CFs and tonotopic organization, and temporal response characteristics. These results are summarized schematically in Figure 15.

The properties described here of neurons in the primary areas, A1 and AAF, which are both located on the MEG, are compatible with previous investigations of these fields (Kelly *et al.*, 1986; Kowalski *et al.*, 1995; Phillips *et al.*, 1988). We have also described auditory cortical fields, located more ventrally on the PEG and AEG, which correspond to the non-primary areas recently identified using optical imaging of intrinsic signals (Nelken *et al.*, 2004). Two of these fields, which we have termed PPF and PSF, are located on the PEG and show some tonotopic order. Neurons in these areas exhibit clear frequency tuning and response thresholds comparable to those recorded in the primary fields, but differ in their temporal response properties. A further two areas are located on the AEG. Neurons in one of these anterior fields (ADF) respond robustly to pure tone stimuli, but show broad, usually high, frequency sensitivity. By contrast, neurons in the more ventral anterior field, AVF, are characterized by poor tone responses and an absence of frequency tuning. Unit thresholds are also considerably higher in this area than in any of the other areas, while neurons in both anterior fields exhibit short latency, transient responses.

As with most other studies of the auditory cortex, these recordings were carried out under anaesthesia and it is possible that the spectrotemporal properties of these neurons may be different in the awake animal. However, the present study emphasizes the differences in response properties that exist over the ferret EG, which provide a basis for subdividing this region into several distinct cortical fields.

A1 and AAF

In the cat, the frequency gradients in A1 and AAF run in almost opposite directions, with the two fields sharing a high-frequency border (Knight, 1977; Reale and Imig, 1980). This is
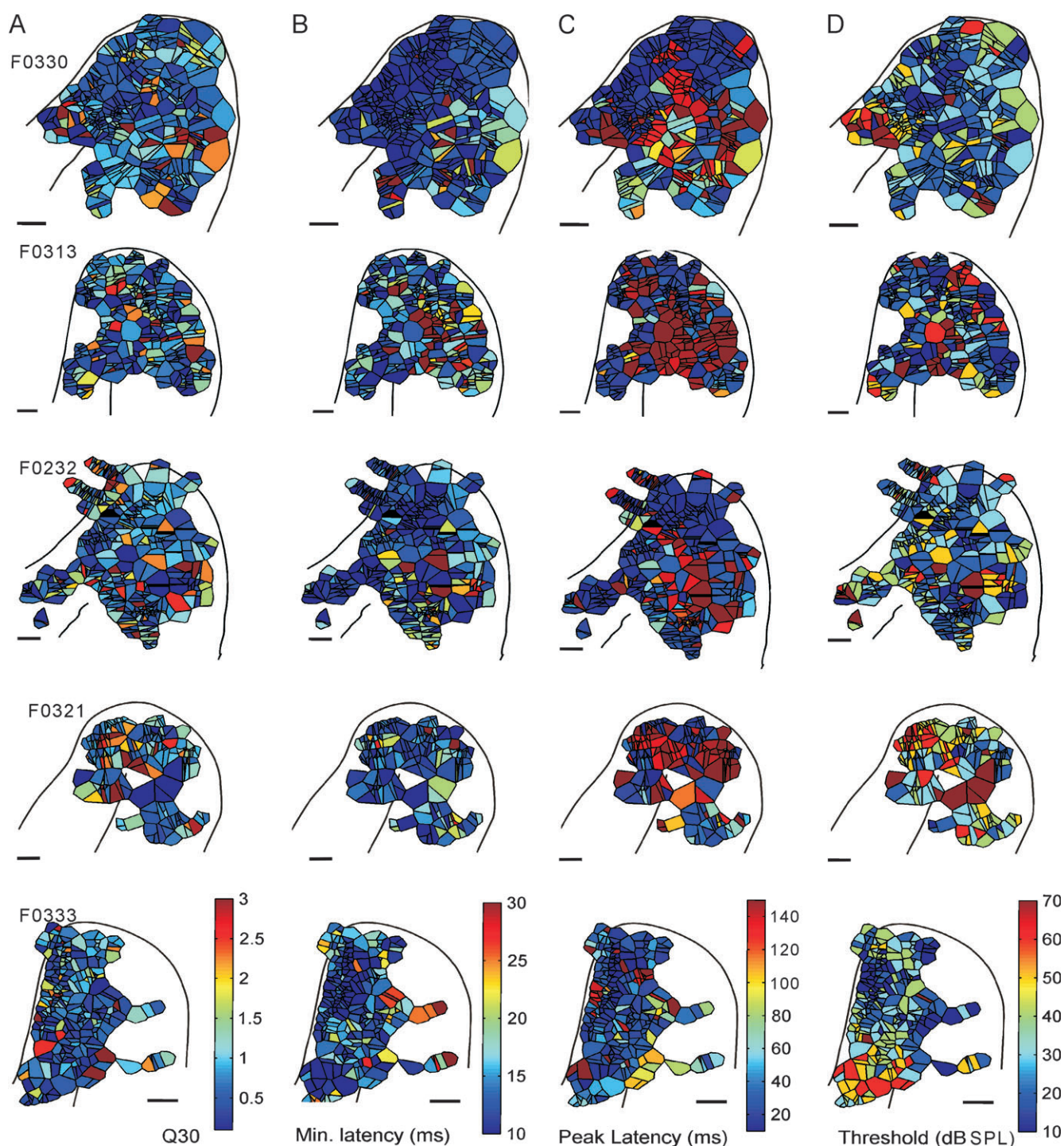
Figure 12. Voronoi tessellation maps illustrating the distribution of Q30 (*A*), minimum response latency (*B*), peak latency (*C*) and unit threshold (*D*) within the ferret auditory cortex. Data from each of the five animals are shown in the different rows.

not the case, however, in the ferret, where a single frequency gradient runs approximately dorsoventrally in the MEG (Kelly *et al.*, 1986; Phillips *et al.*, 1988; Versnel *et al.*, 2002; Nelken *et al.*, 2004). Consequently, previous estimates of the relative regions occupied by A1 and AAF have differed somewhat (Kelly *et al.*, 1986; Pallas *et al.*, 1990; Kowalski *et al.*, 1995).

In keeping with these studies, the distribution of CFs within the MEG failed to reveal a consistent difference between the

frequency representations of A1 and AAF, although there was some indication that the high-to-low-frequency gradients are oriented slightly rostrally for AAF and caudally for A1. Kowalski *et al.* (1995) reported that low-frequency AAF is located on the anterior bank of the ferret's *sss*. In two animals (F0232 and F0333), a number of units were recorded from a corresponding area of the *sss*. In one of them, low-frequency units were indeed found, but in the other one the electrode tracks in the bank of
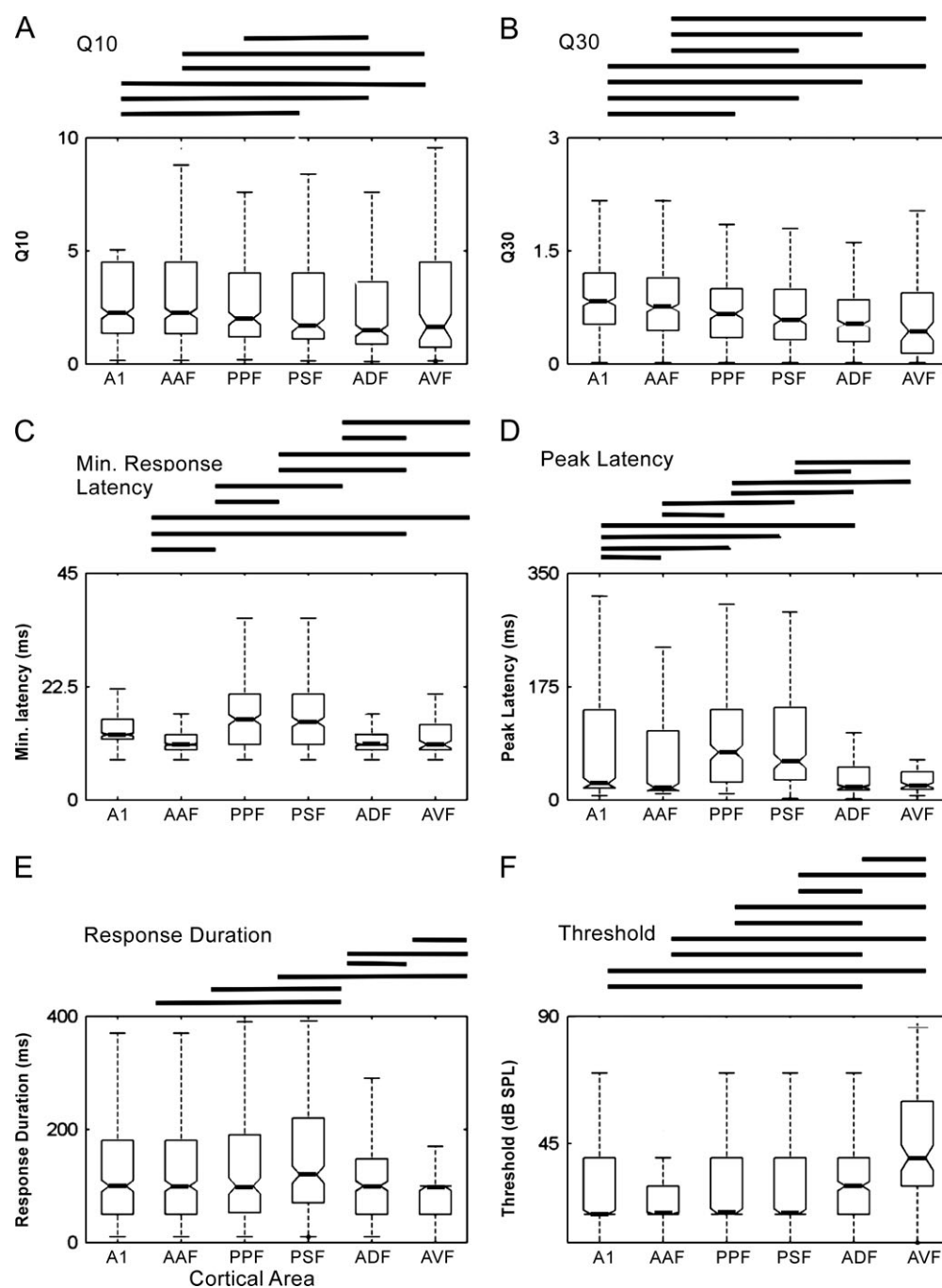
Figure 13. Box plots of the raw data grouped by cortical field (abscissa in each plot) for different response parameters: Q10 (*A*), Q30 (*B*), minimum response latency (*C*), peak latency (*D*), response duration (*E*) and unit threshold (*F*). The boxes extend between the 25th and 75th percentiles (the inter-quartile range), the thick black line is the median and the notch indicates the distribution about the median. The 'whiskers' extending above and below the box show the limits of the remaining percentiles. Values >1.5 times the inter-quartile range were considered to be outliers.

the *sss* encountered only high-frequency units. It is possible that, had we been able to record from this region in all the animals used in this study, we would have found a clearer separation between the frequency representations of the two primary fields. Because we also wished to investigate the non-primary areas in the AEG and PEG, we did not map the better-characterized primary areas to the same degree of detail in all cases. Nevertheless, our recordings suggest that the precise orientation of the frequency gradient in A1 varies somewhat

between animals, in agreement with previous descriptions (Kelly *et al.*, 1986).

Previous comparisons of responses in A1 and AAF, both in ferrets (Kowalski *et al.,* 1995) and other species (Knight, 1977; Phillips and Irvine, 1982; Schreiner and Urbas, 1986; Redies *et al.*, 1989; Thomas *et al.*, 1993; Eggermont, 1998; Linden *et al.*, 2003) have revealed certain differences between them. In keeping with these reports, we found that units classified here as being part of AAF had significantly shorter response

latencies than those in A1. As in the cat (Phillips and Irvine, 1982), guinea pig (Redies *et al.*, 1989; Thomas *et al.*, 1993) and mouse (Linden *et al.*, 2003), we found that the bandwidth of frequency tuning was very similar for the two regions. However, a different result was reported for the ferret by Kowalski *et al.* (1995) and, more recently, for the cat by Imaizumi *et al.* (2004), who found that AAF units were more broadly tuned than those recorded in A1. This difference may reflect the relative under-sampling of the anterior bank of the *sss* in the present study. Like Kowalski *et al.* (1995), we found a comparable range of CFs represented in A1 and AAF (both studies employed essentially the same range of stimulus frequencies). We found that the two

fields differed, however, in the relative magnification of the tonotopic maps. While approximately the same area of cortex was devoted to the representation of different frequencies in A1, we found that the middle frequency range was under represented in AAF (Fig. 9). This has also been observed in AAF in the cat (Imaizumi *et al.*, 2004) and gerbil (Thomas *et al.*, 1993).

Posterior Ectosylvian Gyrus

Our quantitative analysis of the response properties of neurons located in the posterior areas revealed no differences between PPF and PSF. However, the rostrocaudal high–low–high frequency reversal across the PEG argues strongly for the existence of two separate fields, although the precise location of the border between them remains uncertain. Both posterior fields exhibit some tonotopic order, which appears to be arranged dorsoventrally for PPF (Figs 4 and 5) and rostrocaudally for PSF (Figs 4 and 6). Although more detailed sampling will be needed to confirm this, the relatively high Q10 and Q30 values and clear frequency tuning of many PEG neurons, coupled with the cluster sizes for CF, support the idea that there is an ordered frequency representation. Compared with other regions of the EG, PSF and PPF neurons were characterized by long latency responses, multi-peaked PSTHs and non-monotonic responses.

The location of these areas relative to A1 raises the possibility that they may be equivalent to the secondary auditory cortex, A2, and PAF in the cat. An investigation of other responses properties, including sensitivity to sound-source location and to dynamic stimuli, as well as a more detailed analysis of excitatory and inhibitory domains within the FRAs will be needed to confirm such homologies. Nevertheless, it is noteworthy that area PSF, which occupies the posterior region of the PEG, is characterized by neurons with relatively long response latencies, non-monotonic response-level functions, tonotopically organized CFs and often broad frequency tuning, properties that are characteristic of cat PAF neurons (Reale and Imig, 1980; Phillips and Orman, 1984; Phillips *et al.*, 1995; Heil and Irvine, 1998; Tian and Rauschecker, 1998; Loftus and Sutter, 2001; Stecker *et al.*, 2003).

Anterior Ectosylvian Gyrus

We distinguished two further auditory fields on the AEG. In contrast to the other areas characterized in this study, neither of
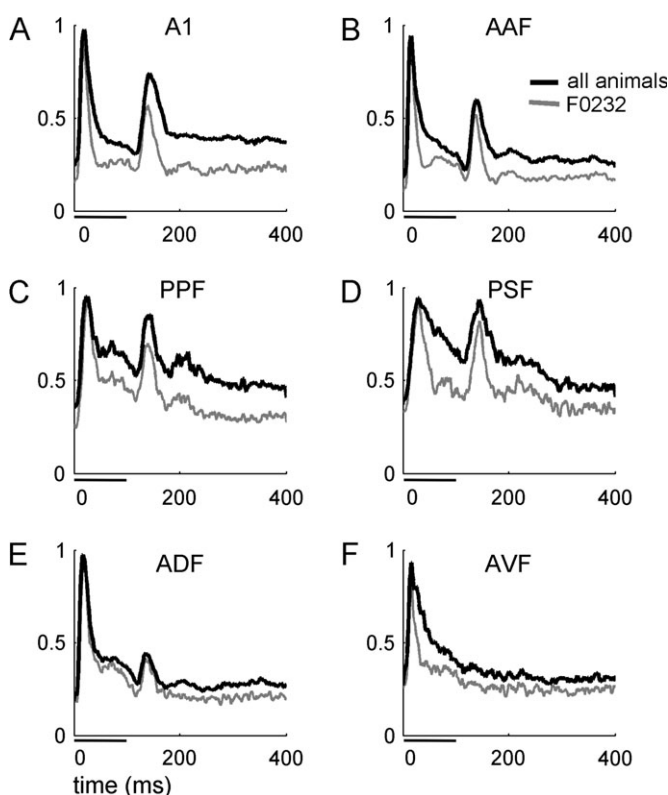

Figure 14. (*A–F*) Variation in temporal firing patterns within the ferret auditory cortex. Black lines: grand average PSTHs constructed by pooling all the normalized PSTHs from each cortical field. Grey lines: data from one animal.

Table 2

Cluster sizes for each response parameter in each of the six cortical fields

Parameter	All areas		A1		AAF		PSF		PPF		ADF		AVF	
CF	7.63		4.2		2.57		0.47		1.16		0.35		0.25	
	3.6	*9.89*	*2.79*	*4.8*	*0.91*	*6.62*	*0*	*4.13*	*0.85*	*2.15*	*0.25*	*3.26*	*0.21*	*0.53*
Q10	1.37		0.59		0.27		0.45		0.67		0.35		0.25	
	0.84	*3.1*	*0.41*	*0.74*	*0.19*	*0.88*	*0*	*2.31*	*0*	*4.59*	*0.18*	*1.96*	*0.21*	*1.5*
Q30	2.06		0		0		0		0		0		0	
	0.84	*9.8*	*0*	*4.77*	*0*	*0.23*	*0*	*1.5*	*0*	*2.92*	*0*	*0.28*	*0*	*0.24*
Min. latency	4.30		0.86		0.76		0.49		0.82		0.73		0.85	
	0.85	*8.2*	*0.41*	*3.25*	*0.24*	*1.45*	*0.18*	*1.37*	*0.04*	*2.3*	*0.25*	*1.62*	*0.26*	*1.61*
Peak latency	2.80		1.09		0.54		1.28		1.48		0.70		0.42	
	6.4	*1.4*	*0.45*	*4.12*	*0.4*	*1.54*	*0*	*1.61*	*0*	*3.58*	*0.53*	*1.54*	*0.21*	*1.38*
Response duration	1.86		0.70		1.09		0.80		0.61		0.36		0.24	
	0.76	*9.1*	*0.39*	*3.03*	*0.4*	*2.57*	*0.14*	*0.63*	*0*	*3.45*	*0.4*	*0.63*	*0.21*	*0.49*

The numbers indicate the median (top row for each parameter) and the 10th and 90th percentile (bottom row for each parameter, italics) values for the cortical distance over which a significant change occurred in the value of the response parameter. See text for details.
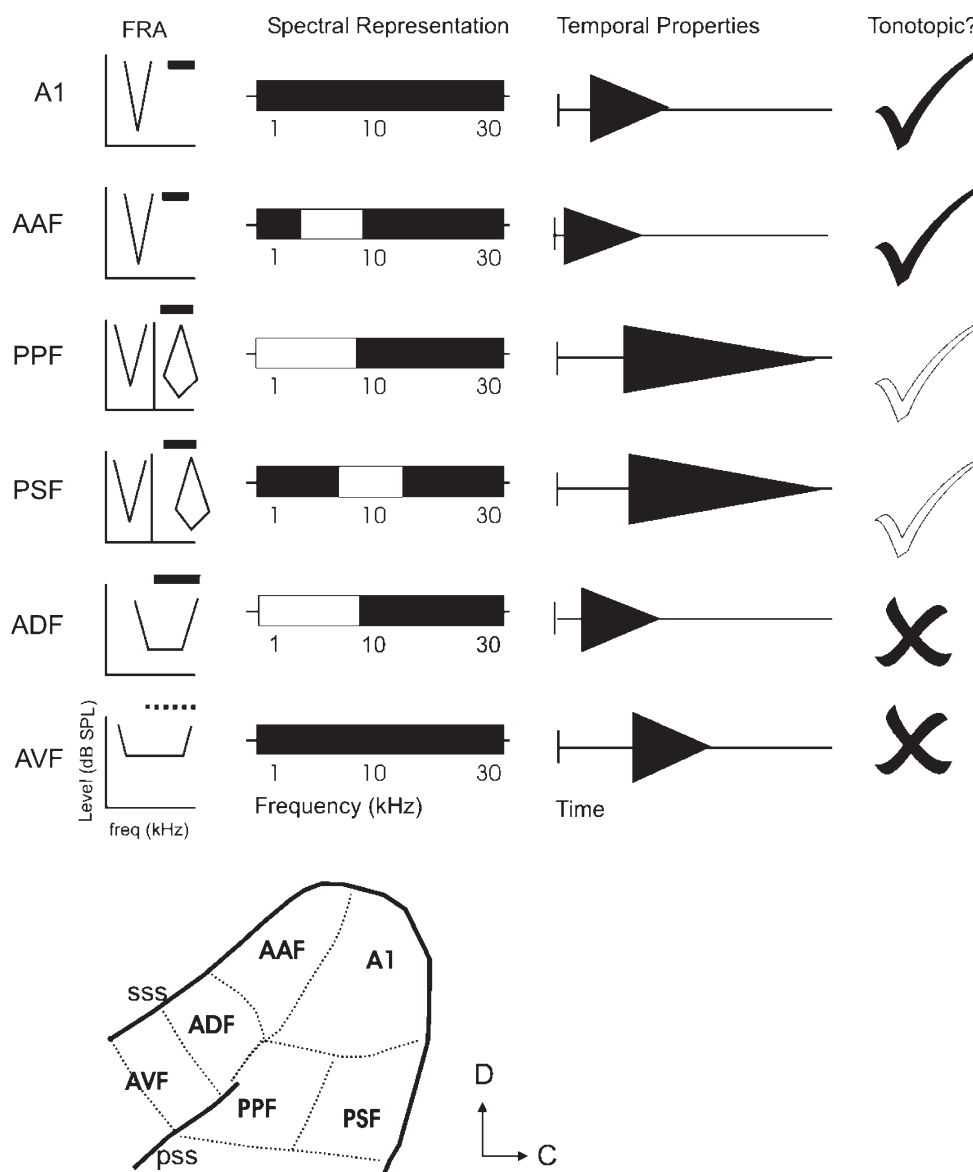
Figure 15. Schematic summarizing the distribution of auditory response properties in each of the six cortical fields characterized in this study. The FRAs (frequency-response areas) depict the relative threshold and shape of the tuning curves for typical units in each area. The width of the bar next to the FRA is an indicator of the relative bandwidth of the tuning curves (the dotted line for field AVF indicates that units in this area frequently responded to noise but not to tones), while the presence of a rhombus denotes a relatively high incidence of non-monotonic response-level functions. The filled spectral representation bars show the range of characteristic frequencies encountered in each field; the open bars indicate that certain frequency ranges were relatively under-represented. The starting position and length of the triangles denote the average response latencies and durations for units recorded in each field.

these anterior fields exhibited any clear tonotopic order and very little clustering of any response property was observed. The minimum response and peak latencies of AEG neurons were comparable to those recorded for neurons in the primary areas. However, their frequency tuning was relatively poor and AEG neurons, particularly in AVF, often responded to broadband noise but not to tones. This location of AVF is close to a multisensory area in the ferret pseudosylvian sulcal cortex, which, on the basis of its visual, auditory and somatosensory responses (M.A. Meredith, personal communication) and connections with other sensory areas of cortex (Ramsay and Meredith, 2004), as well as its inputs to the superior colliculus (Jiang *et al.*, 1996), is thought to be homologous to field AES in the cat; see also Manger *et al.* (2002). Because our recordings

were made on the face of the gyrus, rather than within the *pss*, AVF could be a distinct region of auditory association cortex, although further investigation with stimuli of different sensory modalities will be needed to confirm this.

An Anterior–Posterior Distinction

The purpose of this study was to use spectrally simple sounds to characterize neurons in the ferret EG, with a view to identifying physiologically distinct areas of the auditory cortex. This is a necessary first step, both for extending comparative studies of the functional organization of the cortex to a species that is being used to an increasing extent by auditory researchers, and for future studies of auditory processing and plasticity.

Our data suggest that it is possible to segregate the neurons from which we have recorded into six different areas. Although the primary areas are clearly equivalent to those found in other mammals, establishing cross-species homologies for the four ventral areas will require the use of more complex stimuli and a study of their thalamocortical and corticocortical connectivity. For example, following the recent discovery that cat PAF may have a specialized role in spatial processing (Malhotra *et al.*, 2004; Stecker *et al.*, 2003), it would clearly be of interest to compare the spatial response properties of ferret PSF neurons with those in the other cortical fields.

Our estimation of four non-primary areas is likely to be conservative, particularly as our recordings were typically restricted to the face of the gyri. More detailed sampling of the sulcal regions will be needed in order to characterize the auditory cortex in greater detail. Nevertheless, our data point to clear and consistent differences between areas located on the PEG and those on the AEG. Based on current ideas of auditory information processing in other species (Rauschecker and Tian, 2000; Read *et al.*, 2002; Griffiths *et al.*, 2004), it is possible that these physiological differences between anterior and posterior areas may indicate the existence of task-dependent parallel pathways in the ferret cortex.

Notes

Address correspondence to Dr A.J. King, University Laboratory of Physiology, Parks Road, Oxford OX1 3PT, UK. Email: ajk@physiol.ox.ac.uk.

References

Chapman B, Stryker MP (1993) Development of orientation selectivity in ferret visual cortex and effects of deprivation. J Neurosci 13:5251-5262.

Eggermont JJ (1998) Representation of spectral and temporal sound features in three cortical fields of the cat. Similarities outweigh differences. J Neurophysiol 80:2743-2764.

Fritz J, Shamma S, Elhilali M, Klein D (2003) Rapid task-related plasticity of spectrotemporal receptive fields in primary auditory cortex. Nat Neurosci 6:1216-1223.

Griffiths TD, Warren JD, Scott SK, Nelken I, King AJ (2004) Cortical processing of complex sound: a way forward? Trends Neurosci 27:181-185.

Heil P, Irvine DR (1998) Functional specialization in auditory cortex: responses to frequency-modulated stimuli in the cat's posterior auditory field. J Neurophysiol 79:3041-3059.

Imaizumi K, Priebe NJ, Crum PA, Bedenbaugh PH, Cheung SW, Schreiner CE (2004) Modular functional organization of cat anterior auditory field. J Neurophysiol 92:444-457.

Innocenti GM, Manger PR, Masiello I, Colin I, Tettoni L (2002) Architecture and callosal connections of visual areas 17, 18, 19 and 21 in the ferret (*Mustela putorius*). Cereb Cortex 12:411-422.

Jiang ZD, King AJ, Moore DR, Thompson ID (1996) Auditory cortical projections to the superior colliculus in the ferret. Brit J Audiol 30:109.

Juliano SL, Palmer SL, Sonty RV, Noctor S, Hill GF, 2nd (1996) Development of local connections in ferret somatosensory cortex. J Comp Neurol 374:259-277.

Kavanagh GL, Kelly JB (1987) Contribution of auditory cortex to sound localization by the ferret (*Mustela putorius*). J Neurophysiol 57:1746-1766.

Kelly JB, Judge PW (1994) Binaural organization of primary auditory cortex in the ferret (*Mustela putorius*). J Neurophysiol 71:904-913.

Kelly JB, Judge PW, Phillips DP (1986) Representation of the cochlea in primary auditory cortex of the ferret (*Mustela putorius*). Hear Res 24:111-115.

King AJ, Parsons CH (1999) Improved auditory spatial acuity in visually deprived ferrets. Eur J Neurosci 11:3945-3956.

Kitzes LM, Hollrigel GS (1996) Response properties of units in the posterior auditory field deprived of input from the ipsilateral primary auditory cortex. Hear Res 100:120-130.

Knight PL (1977) Representation of the cochlea within the anterior auditory field (AAF) of the cat. Brain Res 130:447-467.

Kowalski N, Versnel H, Shamma SA (1995) Comparison of responses in the anterior and primary auditory fields of the ferret cortex. J Neurophysiol 73:1513-1523.

Linden JF, Liu RC, Sahani M, Schreiner CE, Merzenich MM (2003) Spectrotemporal structure of receptive fields in areas AI and AAF of mouse auditory cortex. J Neurophysiol 90:2660-2675.

Loftus WC, Sutter ML (2001) Spectrotemporal organization of excitatory and inhibitory receptive fields of cat posterior auditory field neurons. J Neurophysiol 86:475-491.

Malhotra S, Hall AJ, Lomber SG (2004) Cortical control of sound localization in the cat: unilateral cooling deactivation of 19 cerebral areas. J Neurophysiol 92:1625-1643.

Manger PR, Masiello I, Innocenti GM (2002) Areal organization of the posterior parietal cortex of the ferret (*Mustela putorius*). Cereb Cortex 12:1280-1297.

Merzenich MM, Brugge JF (1973) Representation of the cochlear partition of the superior temporal plane of the macaque monkey. Brain Res 50:275-296.

Moore DR, Hine JE, Jiang ZD, Matsuda H, Parsons CH, King AJ (1999) Conductive hearing loss produces a reversible binaural hearing impairment. J Neurosci 19:8704-8711.

Mrsic-Flogel TD, Schnupp JWH, King AJ (2003) Acoustic factors govern developmental sharpening of spatial tuning in the auditory cortex. Nat Neurosci 6:981-988.

Nelken I, Versnel H (2000) Responses to linear and logarithmic frequency-modulated sweeps in ferret primary auditory cortex. Eur J Neurosci 12:549-562.

Nelken I, Bizley JK, Nodal FR, Ahmed B, Schnupp JWH, King AJ (2004) Large-scale organization of ferret auditory cortex revealed using continuous acquisition of intrinsic optical signals. J Neurophysiol 92:2574-2588.

Pallas SL, Roe AW, Sur M (1990) Visual projections induced into the auditory pathway of ferrets. I. Novel inputs to primary auditory cortex (AI) from the LP/pulvinar complex and the topography of the MGN-AI projection. J Comp Neurol 298:50-68.

Phillips DP, Irvine DRF (1982) Properties of single neurons in the anterior auditory field (AAF) of cat cerebral cortex. Brain Res 248:237-244.

Phillips DP, Orman SS (1984) Responses of single neurons in posterior field of cat auditory cortex to tonal stimulation. J Neurophysiol 51:147-163.

Phillips DP, Judge PW, Kelly JB (1988) Primary auditory cortex in the ferret (*Mustela putorius*): neural response properties and topographic organization. Brain Res 443:281-294.

Phillips DP, Semple MN, Kitzes LM (1995) Factors shaping the tone level sensitivity of single neurons in posterior field of cat auditory cortex. J Neurophysiol 73:674-686.

Ramsay AM, Meredith MA (2004) Multiple sensory afferents to ferret pseudosylvian sulcal cortex. Neuroreport 15:461-465.

Rauschecker JP, Tian B (2000) Mechanisms and streams for processing of 'what' and 'where' in auditory cortex. Proc Natl Acad Sci USA 97:11800-11806.

Read HL, Winer JA, Schreiner CE (2002) Functional architecture of auditory cortex. Curr Opin Neurobiol 12:433-440.

Reale RA, Imig TJ (1980) Tonotopic organization in auditory cortex of the cat. J Comp Neurol 192:265-291.

Redies H, Sieben U, Creutzfeldt OD (1989) Functional subdivisions in the auditory cortex of the guinea pig. J Comp Neurol 282:473-488.

Rotman Y, Bar-Yosef O, Nelken I (2001) Relating cluster and population responses to natural sounds and tonal stimuli in cat primary auditory cortex. Hear Res 152:110-127.

Sally SL, Kelly JB (1988) Organization of auditory cortex in the albino rat: sound frequency. J Neurophysiol 59:1627-1638.

Schnupp JWH, Mrsic-Flogel TD, King AJ (2001) Linear processing of spatial cues in primary auditory cortex. Nature 414:200-204.

Schreiner CE, Urbas JV (1986) Representation of amplitude modulation in the auditory cortex of the cat. I. The anterior auditory field (AAF). Hear Res 21:227-241.

Shamma SA, Fleshman JW, Wiser PR, Versnel H (1993) Organization of response areas in ferret primary auditory cortex. J Neurophysiol 69:367-383.

Stecker GC, Mickey BJ, Macpherson EA, Middlebrooks JC (2003) Spatial sensitivity in field PAF of cat auditory cortex. J Neurophysiol 89:2889-2903.

Sur M, Garraghty PE, Roe AW (1988) Experimentally induced visual projections into auditory thalamus and cortex. Science 242:1437-1441.

Sutter ML, Schreiner CE (1991) Physiology and topography of neurons with multipeaked tuning curves in cat primary auditory cortex. J Neurophysiol 65:1207-1226.

Thomas H, Tillein J, Heil P, Scheich H (1993) Functional organization of auditory cortex in the mongolian gerbil (*Meriones unguiculatus*). I. Electrophysiological mapping of frequency representation and distinction of fields. Eur J Neurosci 5:882-897.

Thompson ID, Morgan JE, Henderson Z (1993) The effects of monocular enucleation on ganglion cell number and terminal distribution in the ferret's retinal pathway. Eur J Neurosci 5:357-367.

Tian B, Rauschecker JP (1998) Processing of frequency-modulated sounds in the cat's posterior auditory field. J Neurophysiol 79:2629-2642.

Versnel H, Mossop JE, Mrsic-Flogel TD, Ahmed B, Moore DR (2002) Optical imaging of intrinsic signals in ferret auditory cortex: responses to narrowband sound stimuli. J Neurophysiol 88:1545-1558.

Wallace MN, Roeda D, Harper MS (1997) Deoxyglucose uptake in the ferret auditory cortex. Exp Brain Res 117:488-500.

Woolsey CN, Downman CB, Lende RA (1960) Auditory areas I, II, and Ep: cochlear representation, afferent paths and interconnections. Bull Johns Hopkins Hosp 106:127-142.

Zatorre RJ, Bouffard M, Ahad P, Belin P (2002) Where is 'where' in the human auditory cortex? Nat Neurosci 5:905-909.